Supplementary Materials for Spatio-temporal Bayesian Quantile Regression for High Air-Pollution Concentrations

Edoardo Rosci[1,2*], Jorge Castillo-Mateo[3], Massimo Stafoggia[2], Paola Michelozzi[2], Giovanna Jona Lasinio[1]

[1*]Department of Statistical Sciences, Sapienza University of Rome, Piazzale Aldo Moro 5, Rome, 00185, Italy.
[2]Department of Epidemiology, Lazio Region Health Service/ASL Roma 1, Via Cristoforo Colombo 112, Rome RM, 00147, Italy.
[3]Department of Statistical Methods, University of Zaragoza, Pedro Cerbuna 12, Zaragoza, 50009, Spain.

*Corresponding author(s). E-mail(s): edoardo.rosci@uniroma1.it, e.rosci@deplazio.it;

Keywords: Air pollution, Bayesian modelling, Exposure assessment, Markov chain Monte Carlo, Quantile regression

1 Additional exploratory descriptive analysis

1.1 Temporal patterns

First kind of temporal structure we would like to introduce in the models is the working day and WE/holidays. As shown in Figure 1, such seasonality is especially underlined for NO_2, whilst particulate matter display it only very limited (PM_{10} and $PM_{2.5}$). Figure 2 reports within-year seasonality. All pollutants show higher concentrations during winter and working months, while lower values are usually detected in summer.

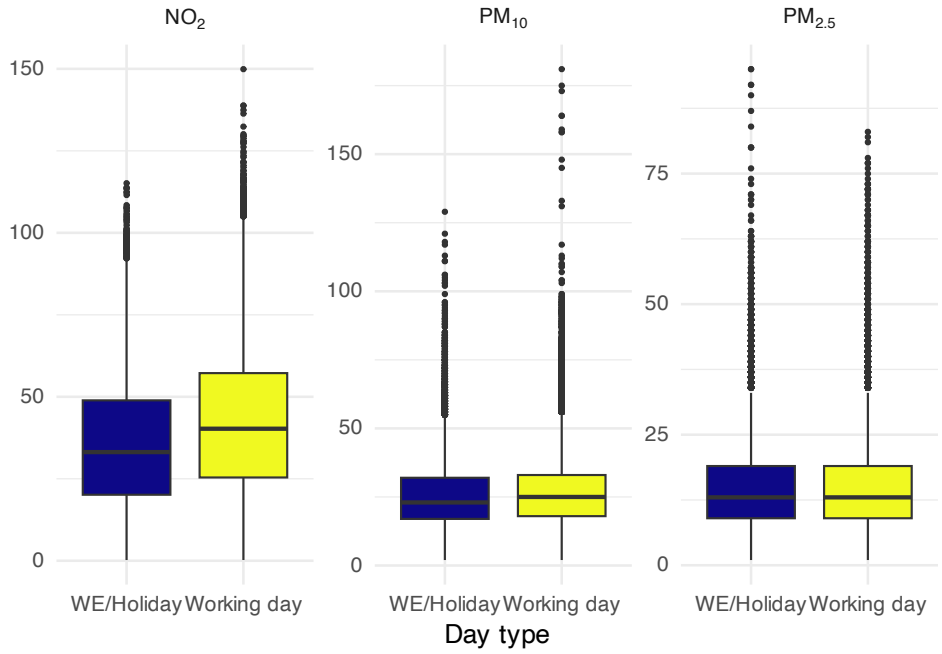

Fig. 1 Boxplots for working days and WE/holidays. Values in $\mu g/m^3$; 2011–2022.

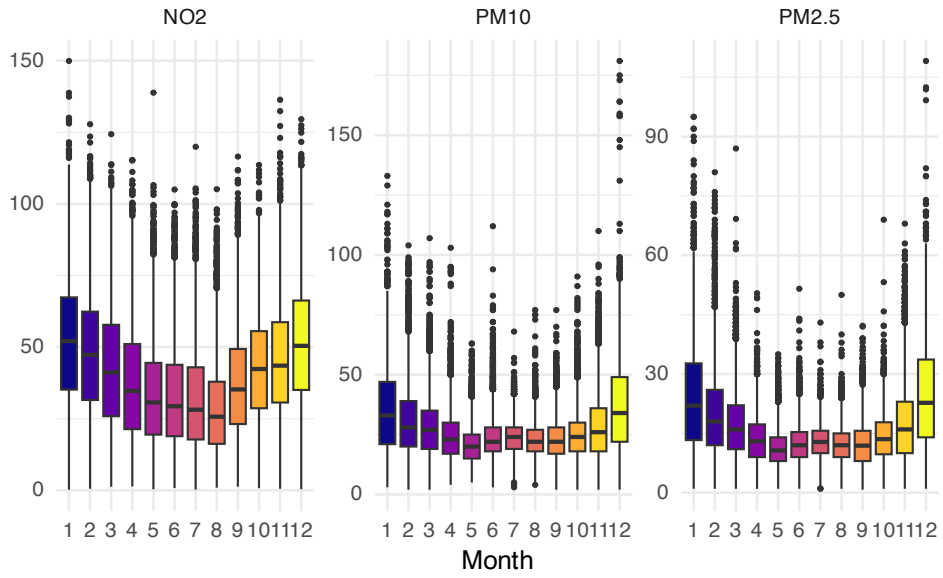

Fig. 2 Boxplots for months. Values in $\mu g/m^3$; 2011–2022.

1.2 Inter-stations distances

As an additional exploratory tool, Table 1 provides the distances between monitoring sites. Among traffic stations, Francia is the most distant from the other traffic sites (nearest traffic neighbour: Tiburtina, 7.77 km). This spatial configuration may partly contribute to the poorer NO_2 LOSO-CV performance at Francia.

2 Additional methodological details

2.1 Additional validation metrics definitions

We provide here an additional validation metric defined for LOSO-CV framework. As well as the ones in the main text, it can be easily extended to the case in which an held-out year is employed, instead of held-out site $\mathbf{s}_i$. The metric is stated in a general form. In the current formalisation the number of years is $T = 12$, and number of days within years is $L = 365$. As well as the other metrics, even this metric can be computed averaging also by number of station as well.

Table 1 Pairwise distances (km) between Rome monitoring stations.

	PRE	FRA	VAD	CDG	CAV	FER	BUF	CIP	MGR	TIB	ARE	MAL	CIN
PRE	0	9.08	5.95	22.86	10.84	6.47	6.88	8.13	2.73	2.76	5.57	16.33	3.87
FRA	9.08	0	3.50	18.06	15.80	9.28	5.32	4.92	7.87	7.77	5.96	13.08	12.93
VAD	5.95	3.50	0	20.55	12.58	8.26	2.76	5.74	5.54	4.29	5.06	14.87	9.80
CDG	22.86	18.06	20.55	0	32.86	17.12	23.11	15.17	20.16	23.57	17.37	6.78	25.36
CAV	10.84	15.80	12.58	32.86	0	17.29	10.55	17.69	13.44	9.35	15.70	26.68	10.92
FER	6.47	9.28	8.26	17.12	17.29	0	10.71	5.05	3.90	8.36	3.37	10.37	8.26
BUF	6.88	5.32	2.76	23.11	10.55	10.71	0	8.49	7.47	4.34	7.68	17.59	10.41
CIP	8.13	4.92	5.74	15.17	17.69	5.05	8.49	0	5.71	8.42	2.69	9.17	11.42
MGR	2.73	7.87	5.54	20.16	13.44	3.90	7.47	5.71	0	4.48	3.04	13.60	5.70
TIB	2.76	7.77	4.29	23.57	9.35	8.36	4.34	8.42	4.48	0	6.36	17.33	6.07
ARE	5.57	5.96	5.06	17.37	15.70	3.37	7.68	2.69	3.04	6.36	0	10.99	8.73
MAL	16.33	13.08	14.87	6.78	26.68	10.37	17.59	9.17	13.60	17.33	10.99	0	18.63
CIN	3.87	12.93	9.80	25.36	10.92	8.26	10.41	11.42	5.70	6.07	8.73	18.63	0

Station codes: ARE = Arenula; BUF = Bufalotta; CAV = Cavaliere; CDG = Castel di Guido; CIN = Cinecitta; CIP = Cipro; FER = Fermi; FRA = Francia; MAL = Malagrotta; MGR = Magna Grecia; PRE = Preneste; TIB = Tiburtina; VAD = Villa Ada

$$R^1_{\text{train}}(\mathbf{s}_i) = 1 - \frac{\sum_{t=1}^{T}\sum_{\ell=1}^{L} \rho_\tau\left(y^{\text{obs}}_{t\ell}(\mathbf{s}_i) - \widehat{q}^{\tau}_{t\ell}(\mathbf{s}_{-i})\right)}{\sum_{t=1}^{T}\sum_{\ell=1}^{L} \rho_\tau\left(y^{\text{obs}}_{t\ell}(\mathbf{s}_i) - q^{\tau}_{\text{emp}}(\mathbf{s}_{-i})\right)} \tag{1}$$

In this case, $\widehat{q}^{\tau}_{t\ell}(\mathbf{s}_{-i})$ is the estimated quantile from the training set evaluated in the training set itself. This metric should be, therefore, slightly more compliant to the training set with respect to the other R^1 specification with different baseline deviance.

2.2 MCMC settings and convergence diagnostics

For each couple (pollutant, τ) two chains of 50,000 iterations were run, plus additional 25,000 burn-in. After 50 thinning, this yielded 2000 iterations (1000 for each chain). Convergence was assessed using (i) trace plots, (ii) potential scale reduction factor ($\hat{R}$), and (iii) effective sample size (ESS), computed with `coda` Rstudio package (Plummer et al. 2006). All parameters were in adequate ranges, with ESS always > 1000 and $\hat{R} < 1.05$. All computations were performed in R on a MacBook Air (Apple M2, 8 GB RAM, macOS). Typical runtime for one tau and one pollutant usually was around 10-20 minutes.

2.3 Kriging details

For each pollutant, model fitting is performed on a transformed response scale, using square-root for NO_2 and $\log(1 + x)$ for particulate matter. Spatial prediction is carried out on the 1 km $\times$ 1 km grid (1292 cells) via Bayesian kriging of the spatial GP-intercept. Since the GP is specified with hierarchical centering representation

$\beta_0^\tau + \mathbf{z}(\mathbf{s})^\top \boldsymbol{\beta}_{sp}^\tau$, kriging is applied to the mean-centred spatial GP and the mean component is added back afterwards, yielding a grid-level estimate of $\beta_0^\tau(\mathbf{s})$. Daily conditional quantile surfaces on the transformed scale are then reconstructed by adding the fixed-effects linear predictor $\mathbf{x}_{t\ell}(\mathbf{s})^\top \boldsymbol{\beta}_{st}^\tau$ (with covariates standardised consistently with model fitting). Final exposure surfaces are reported in $\mu g/m^3$ by applying the inverse transformation, i.e. squaring predictions for NO_2 and exponential minus one for PMs.

3 Model screening

We inspected pairwise correlations computed on the station-level dataset used for fitting the candidate QR models. Pearson correlation coefficients were calculated after preprocessing and standardisation and summarised through correlation matrices (Table 3). We report (i) the correlation structure among spatio-temporal covariates including 1-day lagged terms, and (ii) the correlation matrix among spatial predictors. Pairs showing high absolute correlation ($\mid r \mid \geq 0.75$) were flagged as potentially problematic and removed from the candidate models (Table 2). In addition and for the same reason, at most one spatial predictor was therefore admitted in each model specification. Therefore, candidate models were generated by enumerating all subsets of the spatio-temporal covariates and spatial predictors under such constraints (both with and without station fixed effects). We enumerated a pre-specified grid of 8,192 candidate model specifications sharing a common baseline temporal component $\sin(2\pi\,\text{day}/365) + \cos(2\pi\,\text{day}/365) + \text{year} + \text{day type}$. Final admissible specifications after multi-collinearity checks resulted in 1,500, comprising 1,200 models without station-specific intercepts and 300 models including those (and, hence, without spatial predictors included).

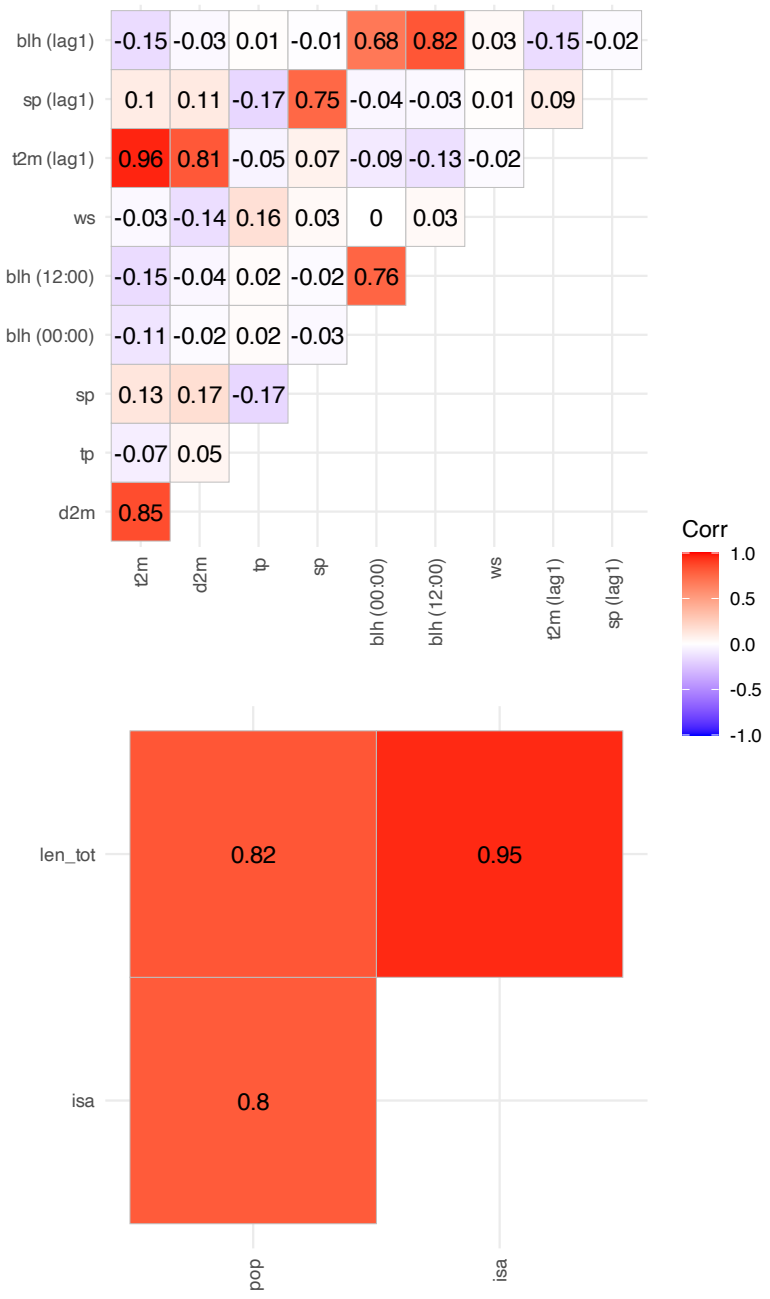

Fig. 3 Correlation matrices among candidate covariates used for multicollinearity screening in model selection.

Table 2 Forbidden covariate pairs excluded from the candidate model set due to high correlation.

Covariate 1	Covariate 2
t2m (mean)	t2m (lag1)
t2m (mean)	d2m (mean)
blh (00:00)	blh (12:00)
blh (12:00)	blh (lag1)
sp (mean)	sp (lag1)

4 Model comparison via DIC

Full spatio-temporal models were evaluated using Deviance Information Criterion (DIC, Spiegelhalter et al. (2002)). DIC is reported here only as a comparative diagnostic to quantify the contribution of model components under the AL working likelihood, and not as a primary model-selection criterion. In sample explanatory qualities of the full model were then compared to several alternative formulations, obtained by selectively removing blocks of predictors (e.g., spatial or temporal covariates) and/or the spatial Gaussian-process component.

In Table 3 we compared models using DIC, for each couple (pollutant, τ). Hence, we considered (M1) full model with GP, (M2) full model without GP, (M3) empty model with GP only, (M4) temporal components-only, with GP, and lastly (M5) full model with GP without spatial covariates included.

In general, the largest reductions in DIC are associated with including the spatial GP component (M1 vs M2) across pollutants and quantile levels. Temporal components also contribute substantially, as shown by the poor fit of the intercept-only GP model (M3). In contrast, removing meteorological covariates yields only modest changes in DIC (M1 vs M4), suggesting a limited incremental contribution beyond the baseline temporal structure and spatial GP. Finally, excluding spatial covariates from the GP mean has a negligible impact (M1 vs M5).

5 Robustness and calibration checks

5.1 Prior sensitivity

In this section, tables for prior sensitivity at $\tau = 0.75, 0.90, 0.95$ are presented. For all couples (pollutant, τ) interpretation are similar to the ones included in the main text for forest plots for $\tau = 0.90$, showing proper overlapping across different parameters and good identifiability.

Table 3 DIC by pollutant and τ.

		DIC				
Pollutant	τ	**M1**	**M2**	**M3**	**M4**	**M5**
NO_2	0.75	163534	209111	201012	163764	163534
NO_2	0.90	178048	217808	216281	178319	178048
NO_2	0.95	190073	225906	228151	190320	190074
PM_{10}	0.75	55924	59259	68688	56410	55925
PM_{10}	0.90	68410	71307	85058	68792	68410
PM_{10}	0.95	79202	82101	95306	79554	79203
$PM_{2.5}$	0.75	47156	48217	59899	47589	47156
$PM_{2.5}$	0.90	52597	53732	71906	53060	52598
$PM_{2.5}$	0.95	57463	58716	78397	57889	57462

Models: M1 = full + GP; M2 = full (no GP); M3 = empty + GP; M4 = trend-only + GP; M5 = full + GP without spatial variables in hierarchical centering.

5.2 In-sample calibration

Table 13 and 14 show additional summaries for in sample computed p metric. In the first output, we provide a brief insight regarding spatial variability: all metrics were computed by grouping stations, reaching always values very close to nominal quantile levels with very low inter-stations variability (the maximum distance is for PM_{10} and $\tau = 0.75$, equal to 0.07). The second table shows aggregated summaries year-wise: we can underline slightly higher variability with respect to the former, especially at $\tau = 0.75$ but, in average, all coverages are close to the nominal level.

5.3 Residual temporal dependence ($\tau = 0.90$)

Residual temporal dependence was assessed via the station-level autocorrelation function of the residual defined as $r_{t\ell}(\mathbf{s}) = \mathbb{I}\{y_{t\ell}(\mathbf{s}) \leq \widehat{q}^{\tau}_{t\ell}(\mathbf{s})\} - \tau$, computed on daily series for $\tau = 0.90$. Across pollutants, the lag 1 autocorrelation represented in Table 15 is moderate (median $\approx$ 0.40–0.49), while the lag-7 autocorrelation is smaller (median $\approx$ 0.13–0.17), indicating daily temporal persistence not fully removed by the included seasonal/trend terms and meteorological covariates. This supports considering a latent spatio-temporal component (e.g., AR evolution of the spatial GP) as a natural extension of the work.

6 Extended CV results

In this section, complete cross-validation results for $\tau = 0.75, 0.90, 0.95$ are provided.

6.1 LOSO CV

Tables 16–18, 19–21, and 22–24 show spatial cross-validation performances across different pollutant and quantiles. Main patterns are consistent with those summarised in

the main text: Francia station shows the poorest performances for $NO2_2$, especially for $\tau = 0.75$.

6.2 LOYO CV

Tables 25–27, 28–30, and 31–33 indicate good temporal predictive performances across pollutants and quantile levels, with median p close to the nominal τ and low year-to-year variability. A small number of held-out years show larger deviations from nominal quantile levels, particularly for NO_2, while PM_{10} and $PM_{2.5}$ remain overall stable.

6.3 FF-LOYO CV

Tables 34–36, 37–39, and 40–42 are mostly consistent with the corresponding LOYO summaries, indicating stable prospective performance in the most recent period (2019–2022). For NO_2, the p metric remains close to nominal across quantile levels, with only modest differences relative to LOYO. For PM_{10} and $PM_{2.5}$, FF-LOYO shows slightly lower calibration in some folds.

7 Additional fixed-effects results

7.1 Re-scaled output ($\tau = 0.90$)

We report in this subsection same fixed-effects outputs as the one in the main text (i.e. the forest plots for year/day type and spatio-temporal components, the table for spatial fixed effects), but re-scaling each covariate by its standard deviation. All values must be referred to transformed response values (square-root for NO_2, $\log(1 + x)$ for PMs).

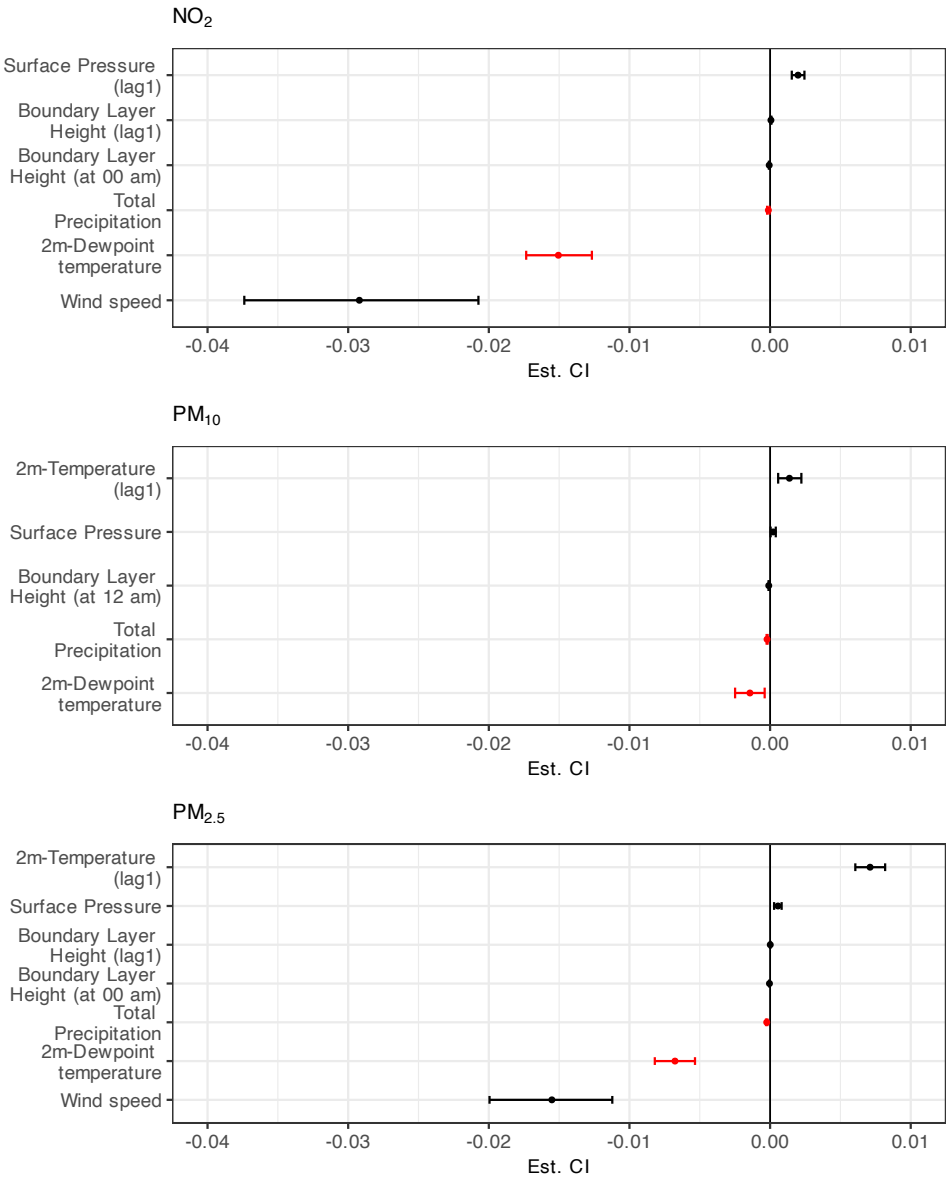

Fig. 4 Estimated 95% credible intervals for fixed effects at $\tau = 0.90$. Responses were transformed (square-root for NO_2; $\log(1 + x)$ for PMs) while covariates were expressed in their original scales. Red markers denote covariates shared by the three best models.

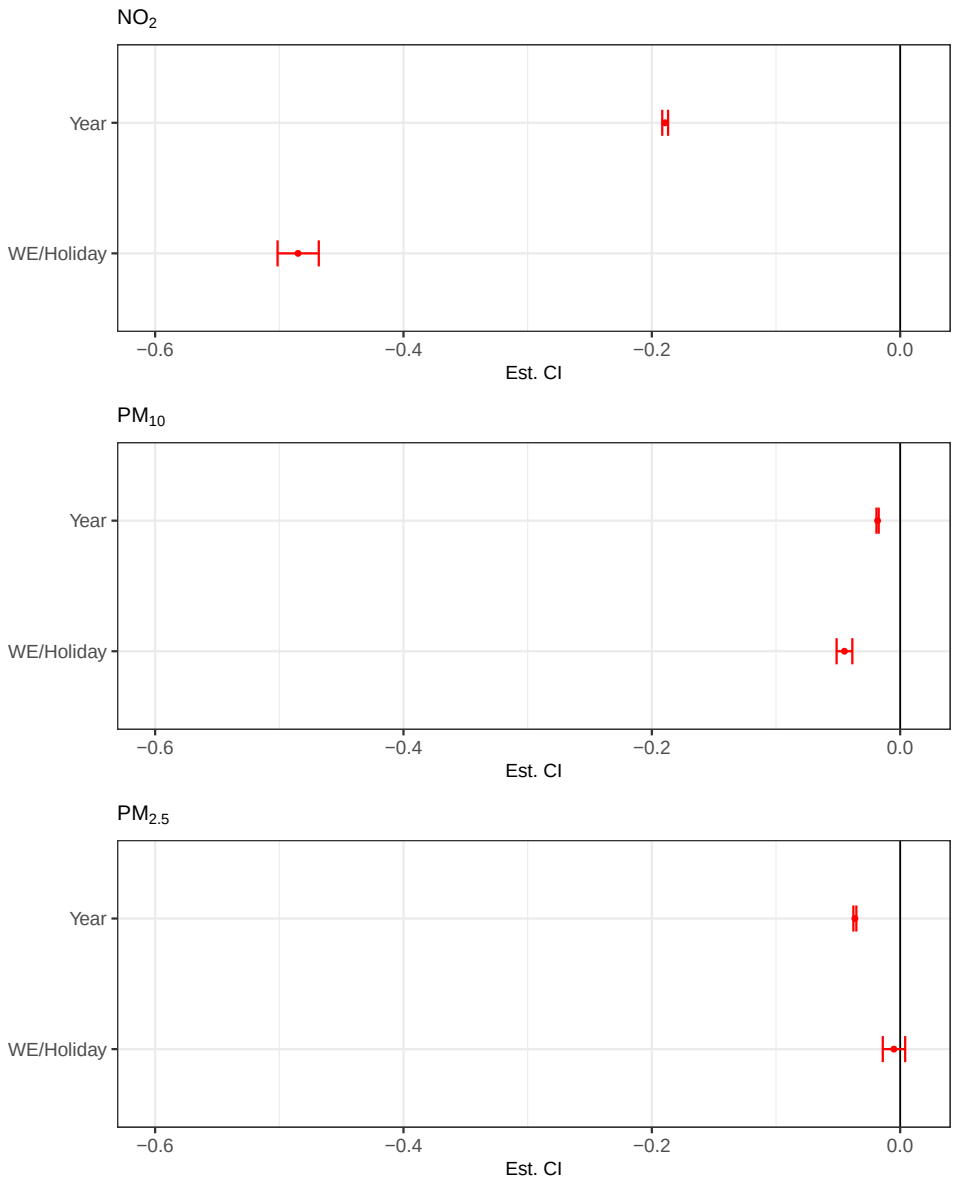

Fig. 5 Estimated 95% credible intervals for year and weekend/holidays temporal components' fixed effects at $\tau = 0.90$. Responses were transformed (square-root for NO_2; $\log(1 + x)$ for PMs) while covariates were expressed in their original scales. All plotted covariates were fixed in the model selection and hence shared by the three best models.

7.2 Fixed-effects summaries

We report here fixed-effect posterior summaries, including in Tables 44–46, 47–49, and 50–52 temporal components, spatio-temporal covariates, and spatial predictors. All results are re-scaled using covariates' standard deviations but are to be referred to transformed response variables (square-root for NO_2 and $\log(1+x)$ for PMs).

Table 4 Prior sensitivity summaries for NO_2 at $\tau = 0.75$ across scenarios.

Param.	**M0**			**MB**			**MS**			**MP**		
	Med	**CI**$_\ell$	**CI**$_u$	**Med**	**CI**$_\ell$	**CI**$_u$	**Med**	**CI**$_\ell$	**CI**$_u$	**Med**	**CI**$_\ell$	**CI**$_u$
β_{d2m}	−0.058	−0.075	−0.041	−0.057	−0.074	−0.041	−0.058	−0.074	−0.041	−0.058	−0.075	−0.040
β_{tp}	−0.017	−0.024	−0.009	−0.017	−0.024	−0.009	−0.017	−0.024	−0.009	−0.017	−0.024	−0.009
σ^τ	0.303	0.300	0.305	0.303	0.300	0.305	0.303	0.300	0.305	0.303	0.300	0.305
ϕ_{β_0}	0.226	0.047	0.660	0.222	0.044	0.659	0.333	0.112	0.753	0.254	0.017	0.844
σ_{β_0}	1.158	0.692	2.482	1.156	0.703	2.556	0.839	0.587	1.355	1.137	0.662	3.426
β_0(CDG)	4.290	4.263	4.318	4.290	4.263	4.319	4.290	4.263	4.318	4.291	4.264	4.318
β_0(MAL)	5.299	5.271	5.332	5.299	5.271	5.326	5.298	5.271	5.328	5.299	5.272	5.328
β_0(CIP)	7.275	7.248	7.301	7.275	7.248	7.302	7.275	7.248	7.302	7.274	7.249	7.301
β_0(MGR)	8.160	8.133	8.185	8.160	8.133	8.188	8.159	8.133	8.185	8.159	8.133	8.190
β_0(FRA)	8.229	8.201	8.258	8.230	8.201	8.264	8.229	8.201	8.262	8.229	8.199	8.263

CI$_\ell$ and CI$_u$ denote the 2.5% and 97.5% quantiles, respectively. Values refer to standardised covariates and the transformed target variable used for model fitting. Covariate codes: d2m = 2 m dewpoint temperature; tp = total precipitation. Station codes: CDG = Castel di Guido; CIP = Cipro; FRA = Francia; MGR = Magna Grecia; MAL = Malagrotta.

Table 5 Prior sensitivity summaries for PM_{10} at $\tau = 0.75$ across scenarios.

Param.	**M0**			**MB**			**MS**			**MP**		
	Med	**CI**$_\ell$	**CI**$_u$	**Med**	**CI**$_\ell$	**CI**$_u$	**Med**	**CI**$_\ell$	**CI**$_u$	**Med**	**CI**$_\ell$	**CI**$_u$
β_{d2m}	−0.023	−0.030	−0.016	−0.023	−0.030	−0.016	−0.023	−0.030	−0.016	−0.023	−0.030	−0.016
β_{tp}	−0.015	−0.018	−0.012	−0.015	−0.018	−0.012	−0.015	−0.018	−0.012	−0.015	−0.018	−0.011
σ^{τ}	0.119	0.118	0.120	0.119	0.118	0.120	0.119	0.118	0.120	0.119	0.118	0.120
ϕ_{β_0}	0.061	0.007	0.326	0.057	0.008	0.318	0.063	0.015	0.280	0.023	0.000	0.245
σ_{β_0}	0.239	0.135	0.587	0.241	0.139	0.580	0.231	0.158	0.385	0.333	0.152	2.263
β_0(CDG)	3.443	3.431	3.455	3.442	3.431	3.453	3.442	3.430	3.454	3.443	3.431	3.454
β_0(MAL)	3.618	3.607	3.630	3.618	3.606	3.630	3.618	3.607	3.630	3.618	3.607	3.629
β_0(CIP)	3.538	3.528	3.548	3.538	3.528	3.549	3.538	3.528	3.549	3.538	3.527	3.548
β_0(MGR)	3.671	3.658	3.681	3.670	3.659	3.681	3.670	3.659	3.682	3.670	3.657	3.681
β_0(FRA)	3.430	3.418	3.439	3.430	3.419	3.440	3.429	3.419	3.440	3.430	3.418	3.440

CI_ℓ and CI_u denote the 2.5% and 97.5% quantiles, respectively. Values refer to standardised covariates and the transformed target variable used for model fitting. Covariate codes: d2m = 2 m dewpoint temperature; tp = total precipitation. Station codes: CDG = Castel di Guido; CIP = Cipro; FRA = Francia; MGR = Magna Grecia; MAL = Malagrotta.

Table 6 Prior sensitivity summaries for $PM_{2.5}$ at $\tau = 0.75$ across scenarios.

Param.	**M0**			**MB**			**MS**			**MP**		
	Med	**CI**$_\ell$	**CI**$_u$	**Med**	**CI**$_\ell$	**CI**$_u$	**Med**	**CI**$_\ell$	**CI**$_u$	**Med**	**CI**$_\ell$	**CI**$_u$
β_{d2m}	−0.045	−0.054	−0.036	−0.045	−0.054	−0.036	−0.045	−0.054	−0.036	−0.045	−0.054	−0.036
β_{tp}	−0.022	−0.026	−0.016	−0.021	−0.027	−0.017	−0.022	−0.027	−0.016	−0.021	−0.026	−0.016
σ^τ	0.139	0.137	0.140	0.139	0.137	0.140	0.139	0.137	0.140	0.139	0.137	0.140
ϕ_{β_0}	0.058	0.005	0.381	0.058	0.007	0.359	0.062	0.011	0.329	0.018	0.001	0.281
σ_{β_0}	0.254	0.144	0.652	0.260	0.147	0.605	0.248	0.166	0.414	0.349	0.162	1.616
β_0(CDG)	2.863	2.849	2.877	2.863	2.849	2.877	2.862	2.849	2.878	2.863	2.850	2.878
β_0(MAL)	2.964	2.951	2.978	2.964	2.950	2.977	2.963	2.950	2.977	2.963	2.949	2.976
β_0(CIP)	2.957	2.944	2.969	2.957	2.944	2.970	2.957	2.943	2.969	2.958	2.945	2.969
β_0(FRA)	3.094	3.083	3.107	3.095	3.082	3.108	3.095	3.082	3.107	3.094	3.082	3.106

CI$_\ell$ and CI$_u$ denote the 2.5% and 97.5% quantiles, respectively. Covariate codes: d2m = 2 m dewpoint temperature; tp = total precipitation. Values refer to standardised covariates and the transformed target variable used for model fitting. Station codes: CDG = Castel di Guido; CIP = Cipro; FRA = Francia; MAL = Malagrotta.

Table 7 Prior sensitivity summaries for NO_2 at $\tau = 0.90$ across scenarios.

Param.	**M0**			**MB**			**MS**			**MP**		
	Med	**CI**$_\ell$	**CI**$_u$	**Med**	**CI**$_\ell$	**CI**$_u$	**Med**	**CI**$_\ell$	**CI**$_u$	**Med**	**CI**$_\ell$	**CI**$_u$
β_{d2m}	−0.088	−0.102	−0.074	−0.087	−0.102	−0.073	−0.088	−0.101	−0.073	−0.088	−0.101	−0.073
β_{tp}	−0.010	−0.018	−0.004	−0.010	−0.018	−0.003	−0.010	−0.019	−0.004	−0.010	−0.018	−0.003
σ^{τ}	0.166	0.164	0.167	0.166	0.164	0.167	0.166	0.164	0.167	0.166	0.164	0.167
ϕ_{β_0}	0.215	0.037	0.623	0.219	0.043	0.685	0.345	0.129	0.738	0.240	0.022	0.887
σ_{β_0}	1.131	0.705	2.546	1.143	0.700	2.440	0.806	0.557	1.259	1.124	0.656	3.205
β_0(CDG)	4.879	4.851	4.907	4.879	4.851	4.907	4.879	4.853	4.909	4.880	4.851	4.910
β_0(MAL)	5.911	5.880	5.937	5.911	5.880	5.939	5.911	5.882	5.936	5.910	5.882	5.940
β_0(CIP)	7.757	7.732	7.783	7.757	7.732	7.782	7.757	7.733	7.781	7.756	7.731	7.781
β_0(MGR)	8.660	8.636	8.685	8.660	8.637	8.683	8.660	8.636	8.686	8.660	8.638	8.684
β_0(FRA)	8.782	8.753	8.809	8.781	8.752	8.807	8.781	8.750	8.809	8.781	8.753	8.808

CI$_\ell$ and CI$_u$ denote the 2.5% and 97.5% quantiles, respectively. Covariate codes: d2m = 2 m dewpoint temperature; tp = total precipitation. Values refer to standardised covariates and the transformed target variable used for model fitting. Station codes: CDG = Castel di Guido; CIP = Cipro; FRA = Francia; MGR = Magna Grecia; MAL = Malagrotta.

Table 8 Prior sensitivity summaries for PM_{10} at $\tau = 0.90$ across scenarios.

Param.	**M0**			**MB**			**MS**			**MP**		
	Med	**CI**$_\ell$	**CI**$_u$	**Med**	**CI**$_\ell$	**CI**$_u$	**Med**	**CI**$_\ell$	**CI**$_u$	**Med**	**CI**$_\ell$	**CI**$_u$
β_{d2m}	−0.009	−0.014	−0.002	−0.008	−0.015	−0.003	−0.009	−0.014	−0.003	−0.009	−0.015	−0.002
β_{tp}	−0.018	−0.021	−0.015	−0.018	−0.021	−0.015	−0.018	−0.021	−0.015	−0.018	−0.021	−0.015
σ^τ	0.065	0.064	0.065	0.065	0.064	0.065	0.065	0.064	0.065	0.065	0.064	0.065
ϕ_{β_0}	0.056	0.006	0.314	0.056	0.007	0.289	0.065	0.016	0.279	0.024	0.002	0.243
σ_{β_0}	0.239	0.14	0.629	0.239	0.134	0.642	0.228	0.153	0.388	0.309	0.149	1.186
β_0(CDG)	3.65	3.64	3.661	3.65	3.639	3.662	3.65	3.639	3.661	3.65	3.639	3.663
β_0(MAL)	3.828	3.817	3.839	3.828	3.818	3.84	3.827	3.817	3.839	3.827	3.818	3.838
β_0(CIP)	3.719	3.71	3.729	3.719	3.71	3.728	3.719	3.711	3.729	3.719	3.711	3.728
β_0(MGR)	3.881	3.871	3.892	3.881	3.871	3.892	3.881	3.87	3.892	3.881	3.871	3.891
β_0(FRA)	3.622	3.611	3.632	3.623	3.611	3.633	3.622	3.612	3.633	3.623	3.612	3.634

CI$_\ell$ and CI$_u$ denote the 2.5% and 97.5% quantiles, respectively. Covariate codes: d2m = 2 m dewpoint temperature; tp = total precipitation. Values refer to standardised covariates and the transformed target variable used for model fitting. Station codes: CDG = Castel di Guido; CIP = Cipro; FRA = Francia; MGR = Magna Grecia; MAL = Malagrotta.

Table 9 Prior sensitivity summaries for $PM_{2.5}$ at $\tau = 0.90$ across scenarios.

Param.	**M0**			**MB**			**MS**			**MP**		
	Med	**CI**$_\ell$	**CI**$_u$	**Med**	**CI**$_\ell$	**CI**$_u$	**Med**	**CI**$_\ell$	**CI**$_u$	**Med**	**CI**$_\ell$	**CI**$_u$
β_{d2m}	−0.039	−0.048	−0.031	−0.039	−0.048	−0.031	−0.039	−0.048	−0.032	−0.039	−0.048	−0.032
β_{tp}	−0.02	−0.024	−0.016	−0.02	−0.024	−0.016	−0.02	−0.024	−0.016	−0.02	−0.024	−0.016
σ^τ	0.072	0.071	0.073	0.072	0.071	0.073	0.072	0.071	0.073	0.072	0.071	0.073
ϕ_{β_0}	0.054	0.006	0.318	0.051	0.005	0.369	0.089	0.015	0.386	0.017	0.001	0.312
σ_{β_0}	0.254	0.143	0.588	0.259	0.146	0.719	0.184	0.123	0.313	0.333	0.153	1.531
β_0(CDG)	3.113	3.1	3.127	3.113	3.101	3.127	3.113	3.1	3.126	3.113	3.101	3.127
β_0(MAL)	3.234	3.222	3.248	3.235	3.221	3.249	3.234	3.22	3.248	3.234	3.219	3.248
β_0(CIP)	3.175	3.163	3.188	3.175	3.163	3.189	3.176	3.162	3.188	3.176	3.164	3.189
β_0(FRA)	3.292	3.281	3.304	3.292	3.282	3.303	3.292	3.282	3.303	3.292	3.282	3.303

CI$_\ell$ and CI$_u$ denote the 2.5% and 97.5% quantiles, respectively. Covariate codes: d2m = 2 m dewpoint temperature; tp = total precipitation. Values refer to standardised covariates and the transformed target variable used for model fitting. Station codes: CDG = Castel di Guido; CIP = Cipro; FRA = Francia; MAL = Malagrotta.

Table 10 Prior sensitivity summaries for NO_2 at $\tau = 0.95$ across scenarios.

Param.	**M0**			**MB**			**MS**			**MP**		
	Med	**CI**$_\ell$	**CI**$_u$	**Med**	**CI**$_\ell$	**CI**$_u$	**Med**	**CI**$_\ell$	**CI**$_u$	**Med**	**CI**$_\ell$	**CI**$_u$
β_{d2m}	−0.084	−0.098	−0.07	−0.085	−0.098	−0.071	−0.084	−0.098	−0.07	−0.084	−0.098	−0.07
β_{tp}	−0.007	−0.014	0	−0.007	−0.014	0.001	−0.007	−0.015	0.001	−0.007	-0.014	0
σ^τ	0.098	0.097	0.098	0.098	0.097	0.098	0.098	0.097	0.098	0.098	0.097	0.098
ϕ_{β_0}	0.213	0.039	0.603	0.221	0.046	0.596	0.339	0.117	0.767	0.256	0.018	0.875
σ_{β_0}	1.137	0.705	2.552	1.115	0.7	2.343	0.795	0.559	1.289	1.098	0.648	3.444
β_0(CDG)	5.182	5.15	5.215	5.182	5.151	5.213	5.183	5.151	5.216	5.182	5.151	5.215
β_0(MAL)	6.263	6.232	6.294	6.264	6.232	6.294	6.264	6.232	6.292	6.264	6.234	6.294
β_0(CIP)	8.009	7.984	8.036	8.01	7.988	8.037	8.01	7.986	8.037	8.01	7.984	8.035
β_0(MGR)	8.946	8.921	8.972	8.947	8.924	8.973	8.946	8.922	8.973	8.947	8.922	8.972
β_0(FRA)	9.105	9.078	9.141	9.106	9.078	9.137	9.106	9.078	9.139	9.105	9.08	9.135

CI$_\ell$ and CI$_u$ denote the 2.5% and 97.5% quantiles, respectively. Covariate codes: d2m = 2 m dewpoint temperature; tp = total precipitation. Values refer to standardised covariates and the transformed target variable used for model fitting. Station codes: CDG = Castel di Guido; CIP = Cipro; FRA = Francia; MGR = Magna Grecia; MAL = Malagrotta.

Table 11 Prior sensitivity summaries for PM_{10} at $\tau = 0.95$ across scenarios.

Param.	**M0**			**MB**			**MS**			**MP**		
	Med	**CI**$_\ell$	**CI**$_u$	**Med**	**CI**$_\ell$	**CI**$_u$	**Med**	**CI**$_\ell$	**CI**$_u$	**Med**	**CI**$_\ell$	**CI**$_u$
β_{t2m}	0.015	0.01	0.022	0.016	0.01	0.022	0.016	0.009	0.022	0.015	0.009	0.022
β_{tp}	−0.018	−0.021	−0.015	−0.018	−0.021	−0.015	−0.018	−0.021	−0.015	−0.018	−0.021	−0.015
σ^{τ}	0.038	0.038	0.038	0.038	0.038	0.038	0.038	0.038	0.038	0.038	0.038	0.038
ϕ_{β_0}	0.05	0.005	0.323	0.05	0.006	0.281	0.057	0.012	0.284	0.019	0.001	0.208
σ_{β_0}	0.242	0.134	0.605	0.236	0.136	0.579	0.225	0.154	0.379	0.342	0.151	1.709
β_0(CDG)	3.786	3.775	3.799	3.787	3.775	3.798	3.787	3.775	3.798	3.786	3.775	3.799
β_0(MAL)	3.984	3.971	3.996	3.984	3.972	3.996	3.985	3.973	3.997	3.984	3.972	3.997
β_0(CIP)	3.848	3.836	3.859	3.847	3.836	3.859	3.848	3.837	3.859	3.848	3.836	3.858
β_0(MGR)	4.013	4.004	4.022	4.014	4.003	4.024	4.013	4.003	4.023	4.013	4.003	4.023
β_0(FRA)	3.758	3.748	3.769	3.758	3.748	3.768	3.757	3.747	3.769	3.758	3.747	3.769

CI$_\ell$ and CI$_u$ denote the 2.5% and 97.5% quantiles, respectively. Covariate codes: t2m = 2 m temperature; tp = total precipitation. Values refer to standardised covariates and the transformed target variable used for model fitting. Station codes: CDG = Castel di Guido; CIP = Cipro; FRA = Francia; MGR = Magna Grecia; MAL = Malagrotta.

Table 12 Prior sensitivity summaries for $PM_{2.5}$ at $\tau = 0.95$ across scenarios.

Param.	**M0**			**MB**			**MS**			**MP**		
	Med	**CI**$_\ell$	**CI**$_u$	**Med**	**CI**$_\ell$	**CI**$_u$	**Med**	**CI**$_\ell$	**CI**$_u$	**Med**	**CI**$_\ell$	**CI**$_u$
β_{d2m}	−0.036	−0.043	-0.028	−0.039	−0.047	−0.032	−0.04	−0.047	−0.032	−0.04	−0.047	−0.032
β_{tp}	−0.022	−0.025	−0.019	−0.02	−0.023	−0.016	−0.019	−0.023	−0.016	−0.02	−0.023	−0.016
σ^τ	0.041	0.041	0.041	0.041	0.04	0.041	0.041	0.041	0.041	0.041	0.041	0.041
ϕ_{β_0}	0.05	0.005	0.372	0.046	0.006	0.306	0.12	0.024	0.444	0.016	0.001	0.263
σ_{β_0}	0.251	0.143	0.669	0.254	0.143	0.649	0.145	0.097	0.241	0.349	0.151	1.459
β_0(CDG)	3.246	3.236	3.258	3.244	3.233	3.255	3.244	3.233	3.255	3.244	3.234	3.255
β_0(MAL)	3.385	3.375	3.396	3.384	3.373	3.395	3.384	3.374	3.396	3.384	3.373	3.396
β_0(CIP)	3.302	3.292	3.313	3.302	3.291	3.313	3.302	3.291	3.314	3.302	3.291	3.313
β_0(FRA)	3.396	3.387	3.406	3.396	3.386	3.408	3.396	3.385	3.406	3.396	3.385	3.407

CI$_\ell$ and CI$_u$ denote the 2.5% and 97.5% quantiles, respectively. Covariate codes: d2m = 2 m dewpoint temperature; tp = total precipitation. Values refer to standardised covariates and the transformed target variable used for model fitting. Station codes: CDG = Castel di Guido; CIP = Cipro; FRA = Francia; MAL = Malagrotta..

Table 13 In-sample calibration check based on the p metric.

Pollutant	τ	$\boldsymbol{p}$
NO_2	0.75	0.750 [0.748, 0.752]
NO_2	0.90	0.900 [0.898, 0.901]
NO_2	0.95	0.950 [0.950, 0.951]
PM_{10}	0.75	0.750 [0.745, 0.757]
PM_{10}	0.90	0.900 [0.898, 0.901]
PM_{10}	0.95	0.950 [0.949, 0.951]
$PM_{2.5}$	0.75	0.750 [0.749, 0.751]
$PM_{2.5}$	0.90	0.900 [0.899, 0.901]
$PM_{2.5}$	0.95	0.950 [0.949, 0.951]

Metric computed station-wise and summarised across stations as median [min, max].

Table 14 In-sample calibration check based on the p metric.

Pollutant	τ	$\boldsymbol{p}$
NO_2	0.75	0.747 (0.702, 0.786) [0.647, 0.876]
NO_2	0.90	0.905 (0.878, 0.916) [0.848, 0.963]
NO_2	0.95	0.952 (0.937, 0.960) [0.919, 0.981]
PM_{10}	0.75	0.748 (0.724, 0.792) [0.670, 0.804]
PM_{10}	0.90	0.898 (0.883, 0.915) [0.862, 0.947]
PM_{10}	0.95	0.950 (0.936, 0.958) [0.932, 0.980]
$PM_{2.5}$	0.75	0.759 (0.723, 0.777) [0.671, 0.821]
$PM_{2.5}$	0.90	0.904 (0.881, 0.921) [0.838, 0.941]
$PM_{2.5}$	0.95	0.952 (0.936, 0.965) [0.913, 0.977]

Metric computed year-wise (2011–2022) and summarised across years as median (Q25, Q75) [min, max].

Table 15 Residual temporal dependence diagnostics for $\tau = 0.90$.

Pollutant	**lag1**	**lag7**
NO_2	0.400 [0.285, 0.593]	0.172
PM_{10}	0.479 [0.379, 0.518]	0.133
$PM_{2.5}$	0.489 [0.458, 0.541]	0.132

Median (and range for lag 1) across monitoring sites of the autocorrelation function (ACF) of the calibration indicator $r_{t\ell}(\mathbf{s}) = \mathbb{I}\{y_{t\ell}(\mathbf{s}) \leq \widehat{q}^{\tau}_{t\ell}(\mathbf{s})\} - \tau$, evaluated at lags 1 and 7 days.

Table 16 LOSO-CV summary for NO_2 at $\tau = 0.75$.

Station	Station Type	τ	R^1	R^1_{train}	WMAE	p
CDG	Background Rural	0.75	−0.273	0.485	4.546	0.980
CAV	Background Suburban	0.75	0.192	0.385	4.516	0.521
MAL	Background Suburban	0.75	0.237	0.552	3.420	0.845
PRE	Background Urban	0.75	0.132	0.154	5.102	0.937
VAD	Background Urban	0.75	−0.334	−0.045	7.368	0.982
BUF	Background Urban	0.75	0.264	0.346	3.648	0.803
CIP	Background Urban	0.75	0.331	0.332	3.802	0.760
ARE	Background Urban	0.75	0.137	0.138	5.053	0.944
CIN	Background Urban	0.75	0.295	0.318	4.307	0.765
FRA	Traffic Urban	0.75	−1.733	−0.838	14.148	0.091
FER	Traffic Urban	0.75	−0.645	0.051	9.319	0.247
MGR	Traffic Urban	0.75	0.081	0.340	5.831	0.451
TIB	Traffic Urban	0.75	−0.179	−0.059	7.243	0.357

WMAE is expressed in $\mu g/m^3$. Station codes: ARE = Arenula; BUF = Bufalotta; CAV = Cavaliere; CDG = Castel di Guido; CIN = Cinecitta; CIP = Cipro; FER = Fermi; FRA = Francia; MAL = Malagrotta; MGR = Magna Grecia; PRE = Preneste; TIB = Tiburtina; VAD = Villa Ada.

Table 17 LOSO-CV summary for PM_{10} at $\tau = 0.75$.

Station	Station Type	τ	R^1	R^1_{train}	WMAE	p
CDG	Background Rural	0.75	−0.094	0.070	3.429	0.819
CAV	Background Suburban	0.75	0.043	0.068	3.696	0.871
MAL	Background Suburban	0.75	0.127	0.167	3.577	0.773
VAD	Background Urban	0.75	0.023	0.066	3.690	0.870
BUF	Background Urban	0.75	0.076	0.080	3.965	0.738
CIP	Background Urban	0.75	0.119	0.122	3.688	0.829
ARE	Background Urban	0.75	0.113	0.113	3.536	0.746
CIN	Background Urban	0.75	0.131	0.149	4.444	0.738
FRA	Traffic Urban	0.75	−0.036	−0.018	4.378	0.502
FER	Traffic Urban	0.75	0.105	0.151	3.611	0.626
MGR	Traffic Urban	0.75	0.174	0.178	3.549	0.775
TIB	Traffic Urban	0.75	0.054	0.125	4.902	0.575

WMAE is expressed in $\mu g/m^3$. Station codes: ARE = Arenula; BUF = Bufalotta; CAV = Cavaliere; CDG = Castel di Guido; CIN = Cinecitta; CIP = Cipro; FER = Fermi; FRA = Francia; MAL = Malagrotta; MGR = Magna Grecia; PRE = Preneste; TIB = Tiburtina; VAD = Villa Ada.

Table 18 LOSO-CV summary for $PM_{2.5}$ at $\tau = 0.75$.

Station	Station Type	τ	R^1	R^1_{train}	WMAE	p
CDG	Background Rural	0.75	0.017	0.088	2.425	0.848
CAV	Background Suburban	0.75	0.193	0.193	2.493	0.796
MAL	Background Suburban	0.75	0.188	0.191	2.876	0.716
VAD	Background Urban	0.75	0.143	0.148	2.534	0.824
CIP	Background Urban	0.75	0.187	0.189	2.512	0.809
ARE	Background Urban	0.75	0.166	0.166	2.443	0.748
CIN	Background Urban	0.75	0.062	0.090	3.552	0.571
FRA	Traffic Urban	0.75	0.103	0.151	2.828	0.590

WMAE is expressed in $\mu g/m^3$. Station codes: ARE = Arenula; BUF = Bufalotta; CAV = Cavaliere; CDG = Castel di Guido; CIN = Cinecitta; CIP = Cipro; FER = Fermi; FRA = Francia; MAL = Malagrotta; MGR = Magna Grecia; PRE = Preneste; TIB = Tiburtina; VAD = Villa Ada.

Table 19 LOSO-CV summary for NO_2 at $\tau = 0.90$.

Station	Station Type	τ	R^1	R^1_{train}	WMAE	p
CDG	Background Rural	0.9	−0.154	0.466	2.490	0.995
CAV	Background Suburban	0.9	0.253	0.361	2.747	0.759
MAL	Background Suburban	0.9	0.255	0.528	1.987	0.944
PRE	Background Urban	0.9	0.146	0.188	2.813	0.985
VAD	Background Urban	0.9	−0.130	0.093	3.755	0.993
BUF	Background Urban	0.9	0.251	0.382	2.079	0.932
CIP	Background Urban	0.9	0.324	0.333	2.122	0.921
ARE	Background Urban	0.9	0.156	0.164	2.812	0.986
CIN	Background Urban	0.9	0.286	0.315	2.525	0.894
FRA	Traffic Urban	0.9	−2.962	−2.151	11.482	0.217
FER	Traffic Urban	0.9	−1.107	−0.352	6.641	0.427
MGR	Traffic Urban	0.9	0.031	0.258	3.366	0.687
TIB	Traffic Urban	0.9	−0.329	−0.256	4.704	0.564

WMAE is expressed in $\mu g/m^3$. Station codes: ARE = Arenula; BUF = Bufalotta; CAV = Cavaliere; CDG = Castel di Guido; CIN = Cinecitta; CIP = Cipro; FER = Fermi; FRA = Francia; MAL = Malagrotta; MGR = Magna Grecia; PRE = Preneste; TIB = Tiburtina; VAD = Villa Ada.

Table 20 LOSO-CV summary for PM_{10} at $\tau = 0.90$.

Station	Station Type	τ	R^1	R^1_{train}	WMAE	p
CDG	Background Rural	0.9	−0.073	0.113	2.130	0.931
CAV	Background Suburban	0.9	0.042	0.065	2.365	0.957
MAL	Background Suburban	0.9	0.170	0.185	2.244	0.900
VAD	Background Urban	0.9	0.076	0.109	2.225	0.956
BUF	Background Urban	0.9	0.091	0.092	2.432	0.887
CIP	Background Urban	0.9	0.170	0.171	2.173	0.933
ARE	Background Urban	0.9	0.152	0.156	2.118	0.895
CIN	Background Urban	0.9	0.169	0.196	2.784	0.876
FRA	Traffic Urban	0.9	0.004	0.015	2.692	0.738
FER	Traffic Urban	0.9	0.155	0.173	2.085	0.857
MGR	Traffic Urban	0.9	0.207	0.212	2.130	0.923
TIB	Traffic Urban	0.9	0.078	0.162	3.082	0.785

WMAE is expressed in $\mu g/m^3$. Station codes: ARE = Arenula; BUF = Bufalotta; CAV = Cavaliere; CDG = Castel di Guido; CIN = Cinecitta; CIP = Cipro; FER = Fermi; FRA = Francia; MAL = Malagrotta; MGR = Magna Grecia; PRE = Preneste; TIB = Tiburtina; VAD = Villa Ada.

Table 21 LOSO-CV summary for $PM_{2.5}$ at $\tau = 0.90$.

Station	Station Type	τ	R^1	R^1_{train}	WMAE	p
CDG	Background Rural	0.9	0.098	0.182	1.461	0.954
CAV	Background Suburban	0.9	0.243	0.243	1.486	0.931
MAL	Background Suburban	0.9	0.252	0.256	1.824	0.861
VAD	Background Urban	0.9	0.229	0.232	1.466	0.935
CIP	Background Urban	0.9	0.260	0.260	1.438	0.936
ARE	Background Urban	0.9	0.235	0.236	1.403	0.895
CIN	Background Urban	0.9	0.123	0.152	2.309	0.751
FRA	Traffic Urban	0.9	0.170	0.182	1.635	0.790

WMAE is expressed in $\mu g/m^3$. Station codes: ARE = Arenula; BUF = Bufalotta; CAV = Cavaliere; CDG = Castel di Guido; CIN = Cinecitta; CIP = Cipro; FER = Fermi; FRA = Francia; MAL = Malagrotta; MGR = Magna Grecia; PRE = Preneste; TIB = Tiburtina; VAD = Villa Ada.

Table 22 LOSO-CV summary for NO_2 at $\tau = 0.95$.

Station	Station Type	τ	R^1	R^1_{train}	WMAE	p
CDG	Background Rural	0.95	−0.142	0.444	1.489	0.998
CAV	Background Suburban	0.95	0.261	0.315	1.762	0.852
MAL	Background Suburban	0.95	0.267	0.512	1.196	0.971
PRE	Background Urban	0.95	0.133	0.195	1.682	0.994
VAD	Background Urban	0.95	−0.014	0.129	2.136	0.995
BUF	Background Urban	0.95	0.227	0.378	1.273	0.978
CIP	Background Urban	0.95	0.313	0.333	1.275	0.968
ARE	Background Urban	0.95	0.175	0.190	1.650	0.995
CIN	Background Urban	0.95	0.268	0.292	1.568	0.939
FRA	Traffic Urban	0.95	−4.245	−3.543	9.018	0.320
FER	Traffic Urban	0.95	−1.367	−0.618	4.461	0.577
MGR	Traffic Urban	0.95	0.003	0.209	2.035	0.812
TIBU	Traffic Urban	0.95	−0.435	−0.363	3.057	0.694

WMAE is expressed in $\mu g/m^3$. Station codes: ARE = Arenula; BUF = Bufalotta; CAV = Cavaliere; CDG = Castel di Guido; CIN = Cinecitta; CIP = Cipro; FER = Fermi; FRA = Francia; MAL = Malagrotta; MGR = Magna Grecia; PRE = Preneste; TIB = Tiburtina; VAD = Villa Ada.

Table 23 LOSO-CV summary for PM_{10} at $\tau = 0.95$.

Station	Station Type	τ	R^1	R^1_{train}	WMAE	p
CDG	Background Rural	0.95	−0.054	0.146	1.346	0.969
CAV	Background Suburban	0.95	0.035	0.063	1.516	0.983
MAL	Background Suburban	0.95	0.168	0.172	1.436	0.939
VAD	Background Urban	0.95	0.093	0.115	1.373	0.980
BUF	Background Urban	0.95	0.073	0.073	1.555	0.945
CIP	Background Urban	0.95	0.169	0.170	1.342	0.963
ARE	Background Urban	0.95	0.151	0.155	1.334	0.952
CIN	Background Urban	0.95	0.153	0.205	1.813	0.928
FRA	Traffic Urban	0.95	0.018	0.023	1.681	0.852
FER	Traffic Urban	0.95	0.145	0.146	1.300	0.938
MGR	Traffic Urban	0.95	0.196	0.197	1.340	0.958
TIB	Traffic Urban	0.95	0.067	0.174	1.958	0.881

WMAE is expressed in $\mu g/m^3$. Station codes: ARE = Arenula; BUF = Bufalotta; CAV = Cavaliere; CDG = Castel di Guido; CIN = Cinecitta; CIP = Cipro; FER = Fermi; FRA = Francia; MAL = Malagrotta; MGR = Magna Grecia; PRE = Preneste; TIB = Tiburtina; VAD = Villa Ada.

Table 24 LOSO-CV summary for $PM_{2.5}$ at $\tau = 0.95$.

Station	**Station Type**	τ	R^1	R^1_{train}	**WMAE**	p
CDG	Background Rural	0.95	0.124	0.208	0.901	0.982
CAV	Background Suburban	0.95	0.249	0.249	0.906	0.963
MAL	Background Suburban	0.95	0.250	0.259	1.177	0.916
VAD	Background Urban	0.95	0.247	0.248	0.878	0.971
CIP	Background Urban	0.95	0.281	0.281	0.844	0.969
ARE	Background Urban	0.95	0.255	0.256	0.831	0.951
CIN	Background Urban	0.95	0.111	0.170	1.523	0.840
FRA	Traffic Urban	0.95	0.216	0.219	0.952	0.890

WMAE is expressed in $\mu g/m^3$. Station codes: ARE = Arenula; BUF = Bufalotta; CAV = Cavaliere; CDG = Castel di Guido; CIN = Cinecitta; CIP = Cipro; FER = Fermi; FRA = Francia; MAL = Malagrotta; MGR = Magna Grecia; PRE = Preneste; TIB = Tiburtina; VAD = Villa Ada.

Table 25 LOYO-CV summary for NO_2 at $\tau = 0.75$.

Year	τ	R^1	R^1_{train}	**WMAE**	p
2011	0.75	0.350	0.516	5.174	0.656
2012	0.75	0.377	0.437	4.751	0.783
2013	0.75	0.336	0.374	4.611	0.774
2014	0.75	0.390	0.390	4.261	0.888
2015	0.75	0.431	0.441	3.896	0.750
2016	0.75	0.426	0.431	3.803	0.700
2017	0.75	0.392	0.398	4.114	0.630
2018	0.75	0.478	0.482	3.274	0.737
2019	0.75	0.379	0.404	3.524	0.673
2020	0.75	0.392	0.477	3.702	0.826
2021	0.75	0.390	0.523	3.157	0.821
2022	0.75	0.345	0.500	3.259	0.719

WMAE is expressed in $\mu g/m^3$.

Table 26 LOYO-CV summary for PM_{10} at $\tau = 0.75$.

Year	τ	$\boldsymbol{R}^1$	$\boldsymbol{R}^1_{\text{train}}$	**WMAE**	$\boldsymbol{p}$
2011	0.75	0.159	0.227	4.125	0.692
2012	0.75	0.113	0.153	3.740	0.699
2013	0.75	0.152	0.153	3.871	0.806
2014	0.75	0.147	0.147	4.092	0.802
2015	0.75	0.138	0.156	4.274	0.665
2016	0.75	0.160	0.161	3.348	0.756
2017	0.75	0.125	0.137	3.237	0.807
2018	0.75	0.149	0.168	2.900	0.798
2019	0.75	0.052	0.079	3.568	0.757
2020	0.75	0.158	0.159	3.791	0.722
2021	0.75	0.027	0.064	3.776	0.737
2022	0.75	0.068	0.085	3.705	0.710

WMAE is expressed in $\mu g/m^3$.

Table 27 LOYO-CV summary for $PM_{2.5}$ at $\tau = 0.75$.

Year	τ	$\boldsymbol{R}^1$	$\boldsymbol{R}^1_{\text{train}}$	**WMAE**	$\boldsymbol{p}$
2011	0.75	0.185	0.321	3.248	0.706
2012	0.75	0.175	0.260	2.749	0.699
2013	0.75	0.154	0.155	3.231	0.780
2014	0.75	0.168	0.168	2.710	0.831
2015	0.75	0.166	0.214	3.314	0.661
2016	0.75	0.192	0.197	2.468	0.768
2017	0.75	0.140	0.149	2.301	0.795
2018	0.75	0.131	0.160	2.016	0.754
2019	0.75	0.000	0.069	2.232	0.762
2020	0.75	0.202	0.206	2.662	0.733
2021	0.75	0.050	0.138	2.193	0.788
2022	0.75	0.101	0.126	2.198	0.660

WMAE is expressed in $\mu g/m^3$.

Table 28 LOYO-CV summary for NO_2 at $\tau = 0.90$.

Year	τ	R^1	R^1_{train}	**WMAE**	p
2011	0.9	0.299	0.518	2.954	0.838
2012	0.9	0.340	0.407	2.730	0.914
2013	0.9	0.267	0.305	2.745	0.898
2014	0.9	0.342	0.342	2.497	0.965
2015	0.9	0.387	0.390	2.203	0.907
2016	0.9	0.375	0.375	2.207	0.879
2017	0.9	0.341	0.341	2.346	0.832
2018	0.9	0.446	0.468	1.829	0.909
2019	0.9	0.335	0.400	2.057	0.861
2020	0.9	0.399	0.474	2.035	0.927
2021	0.9	0.379	0.529	1.777	0.936
2022	0.9	0.309	0.504	1.865	0.869

WMAE is expressed in $\mu g/m^3$.

Table 29 LOYO-CV summary for PM_{10} at $\tau = 0.90$.

Year	τ	R^1	R^1_{train}	**WMAE**	p
2011	0.9	0.214	0.264	2.489	0.870
2012	0.9	0.184	0.197	2.155	0.882
2013	0.9	0.210	0.214	2.352	0.915
2014	0.9	0.187	0.194	2.527	0.906
2015	0.9	0.208	0.243	2.372	0.854
2016	0.9	0.219	0.220	1.935	0.915
2017	0.9	0.136	0.158	1.997	0.928
2018	0.9	0.127	0.167	1.798	0.949
2019	0.9	0.042	0.064	2.327	0.908
2020	0.9	0.209	0.209	2.237	0.871
2021	0.9	0.011	0.045	2.487	0.880
2022	0.9	0.041	0.063	2.416	0.875

WMAE is expressed in $\mu g/m^3$.

Table 30 LOYO-CV summary for $PM_{2.5}$ at $\tau = 0.90$.

Year	τ	$\boldsymbol{R}^1$	$\boldsymbol{R}^1_{\text{train}}$	**WMAE**	$\boldsymbol{p}$
2011	0.9	0.248	0.341	1.953	0.870
2012	0.9	0.238	0.283	1.581	0.902
2013	0.9	0.256	0.279	1.938	0.894
2014	0.9	0.261	0.263	1.555	0.935
2015	0.9	0.225	0.287	1.892	0.825
2016	0.9	0.290	0.290	1.404	0.920
2017	0.9	0.205	0.226	1.366	0.932
2018	0.9	0.201	0.235	1.178	0.943
2019	0.9	0.089	0.184	1.327	0.905
2020	0.9	0.265	0.267	1.540	0.864
2021	0.9	0.100	0.195	1.351	0.910
2022	0.9	0.118	0.172	1.325	0.851

WMAE is expressed in $\mu g/m^3$.

Table 31 LOYO-CV summary for NO_2 at $\tau = 0.95$.

Year	τ	$\boldsymbol{R}^1$	$\boldsymbol{R}^1_{\text{train}}$	**WMAE**	$\boldsymbol{p}$
2011	0.95	0.275	0.533	1.737	0.914
2012	0.95	0.321	0.392	1.643	0.961
2013	0.95	0.219	0.245	1.705	0.942
2014	0.95	0.315	0.315	1.504	0.982
2015	0.95	0.360	0.360	1.311	0.956
2016	0.95	0.341	0.342	1.345	0.940
2017	0.95	0.287	0.288	1.449	0.911
2018	0.95	0.413	0.453	1.113	0.963
2019	0.95	0.294	0.379	1.283	0.928
2020	0.95	0.382	0.466	1.205	0.957
2021	0.95	0.362	0.522	1.065	0.972
2022	0.95	0.282	0.493	1.129	0.928

WMAE is expressed in $\mu g/m^3$.

Table 32 LOYO-CV summary for PM_{10} at $\tau = 0.95$.

Year	τ	$\boldsymbol{R}^1$	$\boldsymbol{R}^1_{\text{train}}$	**WMAE**	$\boldsymbol{p}$
2011	0.95	0.210	0.273	1.601	0.920
2012	0.95	0.214	0.217	1.295	0.950
2013	0.95	0.211	0.220	1.483	0.953
2014	0.95	0.177	0.184	1.632	0.950
2015	0.95	0.189	0.226	1.491	0.922
2016	0.95	0.204	0.205	1.190	0.966
2017	0.95	0.135	0.160	1.260	0.963
2018	0.95	0.082	0.168	1.175	0.981
2019	0.95	−0.003	0.021	1.559	0.949
2020	0.95	0.213	0.214	1.338	0.947
2021	0.95	−0.011	0.020	1.662	0.931
2022	0.95	0.017	0.033	1.602	0.926

WMAE is expressed in $\mu g/m^3$.

Table 33 LOYO-CV summary for $PM_{2.5}$ at $\tau = 0.95$.

Year	τ	$\boldsymbol{R}^1$	$\boldsymbol{R}^1_{\text{train}}$	**WMAE**	$\boldsymbol{p}$
2011	0.95	0.261	0.365	1.188	0.922
2012	0.95	0.260	0.273	0.953	0.952
2013	0.95	0.266	0.308	1.179	0.935
2014	0.95	0.266	0.271	0.920	0.975
2015	0.95	0.229	0.297	1.125	0.904
2016	0.95	0.303	0.304	0.833	0.963
2017	0.95	0.231	0.258	0.834	0.968
2018	0.95	0.187	0.274	0.735	0.980
2019	0.95	0.144	0.238	0.806	0.954
2020	0.95	0.296	0.296	0.885	0.925
2021	0.95	0.112	0.225	0.851	0.949
2022	0.95	0.106	0.195	0.842	0.921

WMAE is expressed in $\mu g/m^3$.

Table 34 FF-LOYO-CV summary for NO_2 at $\tau = 0.75$.

Year	τ	$\boldsymbol{R}^1$	$\boldsymbol{R}^1_{\text{train}}$	**WMAE**	$\boldsymbol{p}$
2019	0.75	0.385	0.456	3.497	0.721
2020	0.75	0.372	0.488	3.848	0.855
2021	0.75	0.385	0.536	3.192	0.821
2022	0.75	0.345	0.500	3.259	0.719

WMAE is expressed in $\mu g/m^3$.

Table 35 FF-LOYO-CV summary for PM_{10} at $\tau = 0.75$.

Year	τ	$\boldsymbol{R}^1$	$\boldsymbol{R}^1_{\text{train}}$	**WMAE**	$\boldsymbol{p}$
2019	0.75	0.041	0.068	3.595	0.721
2020	0.75	0.149	0.153	3.837	0.689
2021	0.75	0.015	0.053	3.818	0.719
2022	0.75	0.068	0.085	3.705	0.710

WMAE is expressed in $\mu g/m^3$.

Table 36 FF-LOYO-CV summary for $PM_{2.5}$ at $\tau = 0.75$.

Year	τ	$\boldsymbol{R}^1$	$\boldsymbol{R}^1_{\text{train}}$	**WMAE**	$\boldsymbol{p}$
2019	0.75	−0.004	0.100	2.227	0.738
2020	0.75	0.199	0.203	2.680	0.717
2021	0.75	0.0504	0.138	2.190	0.764
2022	0.75	0.102	0.127	2.201	0.662

WMAE is expressed in $\mu g/m^3$.

Table 37 FF-LOYO-CV summary for NO_2 at $\tau = 0.90$.

Year	τ	$\boldsymbol{R}^1$	$\boldsymbol{R}^1_{\text{train}}$	**WMAE**	$\boldsymbol{p}$
2019	0.9	0.328	0.430	2.077	0.877
2020	0.9	0.388	0.484	2.079	0.934
2021	0.9	0.377	0.537	1.784	0.931
2022	0.9	0.309	0.504	1.865	0.869

WMAE is expressed in $\mu g/m^3$.

Table 38 FF-LOYO-CV summary for PM_{10} at $\tau = 0.90$.

Year	τ	$\boldsymbol{R}^1$	$\boldsymbol{R}^1_{\text{train}}$	**WMAE**	$\boldsymbol{p}$
2019	0.9	0.019	0.051	2.353	0.862
2020	0.9	0.188	0.189	2.313	0.842
2021	0.9	−0.007	0.027	2.527	0.863
2022	0.9	0.041	0.063	2.416	0.875

WMAE is expressed in $\mu g/m^3$.

Table 39 FF-LOYO-CV summary for $PM_{2.5}$ at $\tau = 0.90$.

Year	τ	R^1	R^1_{train}	**WMAE**	p
2019	0.9	0.064	0.198	1.344	0.856
2020	0.9	0.248	0.254	1.594	0.845
2021	0.9	0.097	0.210	1.353	0.898
2022	0.9	0.118	0.172	1.325	0.851

WMAE is expressed in $\mu g/m^3$.

Table 40 FF-LOYO-CV summary for NO_2 at $\tau = 0.95$.

Year	τ	R^1	R^1_{train}	**WMAE**	p
2019	0.95	0.280	0.399	1.306	0.926
2020	0.95	0.371	0.473	1.230	0.962
2021	0.95	0.358	0.527	1.074	0.969
2022	0.95	0.282	0.493	1.129	0.927

WMAE is expressed in $\mu g/m^3$.

Table 41 FF-LOYO-CV summary for PM_{10} at $\tau = 0.95$.

Year	τ	R^1	R^1_{train}	**WMAE**	p
2019	0.95	−0.054	-0.019	1.608	0.919
2020	0.95	0.185	0.185	1.416	0.913
2021	0.95	−0.050	-0.008	1.716	0.917
2022	0.95	0.017	0.033	1.602	0.926

WMAE is expressed in $\mu g/m^3$.

Table 42 FF-LOYO-CV summary for $PM_{2.5}$ at $\tau = 0.95$.

Year	τ	R^1	R^1_{train}	**WMAE**	p
2019	0.95	0.106	0.233	0.823	0.918
2020	0.95	0.261	0.262	0.961	0.900
2021	0.95	0.104	0.231	0.858	0.940
2022	0.95	0.106	0.195	0.842	0.922

WMAE is expressed in $\mu g/m^3$.

Table 43 Estimated 95% credible intervals for spatial fixed effects in the spatial random process ($\tau = 0.90$)

Pollutant	**Parameter**	**Median**	**2.5%**	**97.5%**
NO_2	Imperviousness Surface Areas	0.209	−0.058	0.452
PM_{10}	Population	0.0056	−0.016	0.028
$PM_{2.5}$	Population	0.00096	−0.023	0.026

Responses were transformed (square-root for NO_2; $\log(1 + x)$ for PMs) while covariates were expressed in their original scales.

Table 44 Fixed-effect posterior summaries for NO_2 at $\tau = 0.75$, reported as posterior median (2.5%, 97.5%).

Covariate	**Median (2.5%, 97.5%)**
Daily seasonality (sin.)	0.044 (0.029, 0.060)
Daily seasonality (cos.)	0.851 (0.831, 0.872)
Year	−0.175 (−0.177, −0.172)
Weekend/holiday	−0.514 (−0.530, −0.498)
2m Dewpoint temperature	-9.90×10^{-3} (-1.29×10^{-2}, -7.04×10^{-3})
Total precipitation	-2.00×10^{-4} (-2.90×10^{-4}, -1.04×10^{-4})
Surface pressure	2.07×10^{-3} (1.60×10^{-3}, 2.54×10^{-3})
Boundary layer height (12:00)	-6.60×10^{-5} (-1.01×10^{-4}, -3.23×10^{-5})
Wind speed	-2.26×10^{-2} (-3.11×10^{-2}, -1.42×10^{-2})
2m Temperature (lag 1)	-5.26×10^{-3} (-7.40×10^{-3}, -3.12×10^{-3})
Imperviousness surface areas	0.224 (−0.048, 0.457)

Table 45 Fixed-effect posterior summaries for PM_{10} at $\tau = 0.75$, reported as posterior median (2.5%, 97.5%).

Covariate	**Median (2.5%, 97.5%)**
Daily seasonality (sin.)	0.050 (0.044, 0.056)
Daily seasonality (cos.)	0.259 (0.251, 0.268)
Year	−0.022 (−0.023, −0.021)
Weekend/holiday	−0.058 (−0.064, −0.052)
2m Dewpoint temperature	-3.94×10^{-3} (-5.14×10^{-3}, -2.77×10^{-3})
Total precipitation	-1.78×10^{-4} (-2.17×10^{-4}, -1.37×10^{-4})
Surface pressure	4.09×10^{-4} (2.18×10^{-4}, 6.01×10^{-4})
Boundary layer height (12:00)	-7.16×10^{-5} (-8.42×10^{-5}, -5.86×10^{-5})
Wind speed	-7.86×10^{-3} (-1.11×10^{-2}, -4.39×10^{-3})
2m Temperature (lag 1)	4.97×10^{-3} (4.15×10^{-3}, 5.75×10^{-3})
Population	0.006 (−0.016, 0.029)

Table 46 Fixed-effect posterior summaries for $PM_{2.5}$ at $\tau = 0.75$, reported as posterior median (2.5%, 97.5%).

Covariate	**Median (2.5%, 97.5%)**
Daily seasonality (sin.)	0.054 (0.044, 0.063)
Daily seasonality (cos.)	0.361 (0.349, 0.373)
Year	−0.037 (−0.038, −0.036)
Weekend/holiday	−0.010 (−0.019, −0.002)
2m Dewpoint temperature	-8.00×10^{-3} (-9.00×10^{-3}, -6.00×10^{-3})
Total precipitation	-2.58×10^{-4} (-3.14×10^{-4}, -1.92×10^{-4})
Surface pressure	8.95×10^{-4} (6.19×10^{-4}, 1.00×10^{-3})
Boundary layer height (12:00)	-6.25×10^{-5} (-8.13×10^{-5}, -4.44×10^{-5})
Wind speed	−0.019 (−0.024, −0.014)
2m Temperature (lag 1)	0.007 (0.006, 0.008)
Population	-1.77×10^{-4} (−0.030, 0.034)

Table 47 Fixed-effect posterior summaries for NO_2 at $\tau = 0.90$, reported as posterior median (2.5%, 97.5%).

Covariate	**Median (2.5%, 97.5%)**
Daily seasonality (sin.)	0.072 (0.058, 0.086)
Daily seasonality (cos.)	0.897 (0.879, 0.915)
Year	−0.189 (−0.192, −0.187)
Weekend/holiday	−0.485 (−0.501, −0.468)
2m Dewpoint temperature	−0.015 (−0.017, −0.013)
Total precipitation	-1.23×10^{-4} (-2.12×10^{-4}, -4.07×10^{-5})
Boundary layer height (00:00)	-6.30×10^{-5} (-8.77×10^{-5}, -3.75×10^{-5})
Wind speed	−0.029 (−0.037, −0.021)
Surface pressure	0.002 (0.002, 0.002)
Boundary layer height (lag 1)	6.01×10^{-5} (2.79×10^{-5}, 9.60×10^{-5})
Imperviousness surface areas	0.217 (−0.058, 0.452)

Table 48 Fixed-effect posterior summaries for PM_{10} at $\tau = 0.90$, reported as posterior median (2.5%, 97.5%).

Covariate	**Median (2.5%, 97.5%)**
Daily seasonality (sin.)	0.051 (0.044, 0.057)
Daily seasonality (cos.)	0.279 (0.271, 0.287)
Year	−0.018 (−0.019, −0.017)
Weekend/holiday	−0.045 (−0.051, −0.039)
2m Dewpoint temperature	-0.001 (-0.002, -3.86×10^{-4})
Total precipitation	-2.17×10^{-4} (-2.48×10^{-4}, -1.76×10^{-4})
Surface pressure	2.23×10^{-4} (3.79×10^{-5}, 4.04×10^{-4})
Boundary layer height (12:00)	-9.49×10^{-5} (-1.08×10^{-4}, -8.05×10^{-5})
2m Temperature (lag 1)	0.001 (5.73×10^{-4}, 0.002)
Population	0.005 (−0.016, 0.029)

Table 49 Fixed-effect posterior summaries for $PM_{2.5}$ at $\tau = 0.90$, reported as posterior median (2.5%, 97.5%).

Covariate	**Median (2.5%, 97.5%)**
Daily seasonality (sin.)	0.063 (0.054, 0.072)
Daily seasonality (cos.)	0.424 (0.414, 0.434)
Year	−0.036 (−0.038, −0.035)
Weekend/holiday	−0.005 (−0.014, 0.004)
2m Dewpoint temperature	−0.007 (−0.008, −0.005)
Total precipitation	-2.40×10^{-4} (-2.88×10^{-4}, -1.92×10^{-4})
Surface pressure	5.62×10^{-4} (2.86×10^{-4}, 8.20×10^{-4})
Boundary layer height (00:00)	-4.50×10^{-5} (-5.83×10^{-5}, -3.15×10^{-5})
Wind speed	−0.016 (−0.020, −0.011)
2m Temperature (lag 1)	0.007 (0.006, 0.008)
Boundary layer height (lag 1)	1.17×10^{-5} (-7.34×10^{-6}, 3.12×10^{-5})
Population	4.74×10^{-4} (−0.031, 0.030)

Table 50 Fixed-effect posterior summaries for NO_2 at $\tau = 0.95$, reported as posterior median (2.5%, 97.5%).

Covariate	**Median (2.5%, 97.5%)**
Daily seasonality (sin.)	0.102 (0.087, 0.116)
Daily seasonality (cos.)	0.891 (0.873, 0.910)
Year	−0.199 (−0.201, −0.197)
Weekend/holiday	−0.464 (−0.480, −0.448)
2m Dewpoint temperature	-1.44×10^{-2} (-1.68×10^{-2}, -1.20×10^{-2})
Total precipitation	-8.74×10^{-5} (-1.72×10^{-4}, 7.88×10^{-6})
Boundary layer height (00:00)	-9.63×10^{-5} (-1.21×10^{-4}, -6.84×10^{-5})
Wind speed	-2.20×10^{-2} (-2.98×10^{-2}, -1.45×10^{-2})
Surface pressure (lag 1)	1.67×10^{-3} (1.25×10^{-3}, 2.11×10^{-3})
Boundary layer height (lag 1)	1.05×10^{-4} (7.05×10^{-5}, 1.39×10^{-4})
Imperviousness surface areas	0.218 (−0.047, 0.438)

Table 51 Fixed-effect posterior summaries for PM_{10} at $\tau = 0.95$, reported as posterior median (2.5%, 97.5%).

Covariate	**Median (2.5%, 97.5%)**
Daily seasonality (sin.)	0.051 (0.044, 0.057)
Daily seasonality (cos.)	0.279 (0.271, 0.287)
Year	−0.018 (−0.019, −0.017)
Weekend/holiday	−0.045 (−0.051, −0.039)
2m Dewpoint temperature	-1.43×10^{-3} (-2.49×10^{-3}, -3.86×10^{-4})
Total precipitation	-2.17×10^{-4} (-2.48×10^{-4}, -1.76×10^{-4})
Surface pressure	2.23×10^{-4} (3.79×10^{-5}, 4.04×10^{-4})
Boundary layer height (12:00)	-9.49×10^{-5} (-1.08×10^{-4}, -8.05×10^{-5})
2m Temperature (lag 1)	1.38×10^{-3} (5.73×10^{-4}, 2.22×10^{-3})
Population	0.005 (−0.016, 0.029)

Table 52 Fixed-effect posterior summaries for $PM_{2.5}$ at $\tau = 0.95$, reported as posterior median (2.5%, 97.5%).

Covariate	**Median (2.5%, 97.5%)**
Daily seasonality (sin.)	0.069 (0.060, 0.078)
Daily seasonality (cos.)	0.427 (0.416, 0.437)
Year	−0.036 (−0.037, −0.035)
Weekend/holiday	-5.48×10^{-3} (-1.33×10^{-2}, 2.34×10^{-3})
2m Dewpoint temperature	-6.17×10^{-3} (-7.39×10^{-3}, -4.94×10^{-3})
Total precipitation	-2.64×10^{-4} (-3.04×10^{-4}, -2.27×10^{-4})
Surface pressure	5.82×10^{-4} (3.78×10^{-4}, 7.87×10^{-4})
Boundary layer height (00:00)	-5.26×10^{-5} (-6.50×10^{-5}, -3.99×10^{-5})
2m Temperature (lag 1)	5.52×10^{-3} (4.57×10^{-3}, 6.52×10^{-3})
Boundary layer height (lag 1)	2.07×10^{-5} (4.40×10^{-6}, 3.73×10^{-5})
Population	0.002 (−0.026, 0.032)

8 Additional results for exposure surfaces

8.1 Relationships between analysed quantile levels

To assess whether focusing on $\tau = 0.90$ is representative, we computed Pearson correlations between posterior mean GP-intercept surfaces across quantile levels (Table 53 and 54). Both the posterior mean GP-intercept surfaces and the annual-average posterior mean quantile surfaces are highly similar across τ, with correlations very close to 1 for NO_2 and ≥ 0.96 for PM_{10}. For $PM_{2.5}$, correlations remain high but are lower for the (0.75, 0.95) pair.

Table 53 Pearson correlations between posterior mean GP-intercept surfaces across quantile levels.

Pollutant	**corr**(0.75, 0.90)	**corr**(0.90, 0.95)	**corr**(0.75, 0.95)
NO_2	0.999	1.000	0.999
PM_{10}	0.988	0.986	0.961
$PM_{2.5}$	0.932	0.976	0.848

Metrics computed over the 1 km grid cells ($n = 1292$).

8.1.1 Quantile crossing

We assessed quantile crossing on the prediction grid by checking, for each day (2011–2022) and each of the 1292 cells, whether the posterior mean surfaces satisfied $\widehat{q}^{0.75}_{t\ell}(\mathbf{s}) \leq \widehat{q}^{0.90}_{t\ell}(\mathbf{s}) \leq \widehat{q}^{0.95}_{t\ell}(\mathbf{s}),\ \forall \mathbf{s}, t, \ell$. As expected, since considered levels are quite distant, no crossings were observed for any pollutant (0 violations across all grid–day combinations).

Table 54 Pearson correlations between annual-average posterior mean τ-quantile surfaces across quantile levels.

Year	Pollutant	corr(0.75, 0.90)	corr(0.90, 0.95)	corr(0.75, 0.95)
2011	NO_2	1.000	1.000	1.000
2011	PM_{10}	1.000	1.000	1.000
2011	$PM_{2.5}$	0.944	0.980	0.873
2022	NO_2	1.000	1.000	1.000
2022	PM_{10}	1.000	1.000	1.000
2022	$PM_{2.5}$	0.968	0.987	0.924

Metrics computed over the 1 km grid cells ($n = 1292$) in 2011 and 2022.

8.2 Observed-predicted agreement ($\tau = 0.90$)

Figure 6 and Table 55 provide a diagnostic for $\tau = 0.90$, comparing each station by observed and predicted quantiles. Specifically, for each pollutant and year (2011, 2022), we compare (i) the observed empirical annual quantile of level $\tau = 0.90$ of daily mean concentrations at each station, $q_{\text{obs}}^{0.90}$, with (ii) an annual summary of the model output, $\widehat{q}_{\text{pred}}^{0.90}$, obtained as the empirical annual 90-th quantile of the day-specific conditional $\tau = 0.90$ estimates evaluated at the corresponding station grid cell. While these two quantities are not identical estimands, their comparison is intended as a qualitative calibration check to assess whether observed stations empirical upper-tail behaviours are in accordance with the fitted quantile models.

For NO_2, the scatter indicates a strong concordance in both years, with a slight tendency to overpredict the annual upper-tail level, more evident in 2011 and particularly for traffic sites. For PM_{10}, station concordance seems preserved, but the comparison suggests an overestimation of the annual $\tau = 0.90$ quantile (especially in 2011). Lastly, for $PM_{2.5}$, agreement is weaker probably due to the sparse monitoring network, and the diagnostic highlights a clear positive overestimation in 2011 (and a smaller one in 2022). Table 55 summarises these patterns by reporting the median and range (min–max) of $q_{\text{pred}} - q_{\text{obs}}$ across sites for each pollutant and year, confirming an overall positive bias under the adopted annual aggregation.

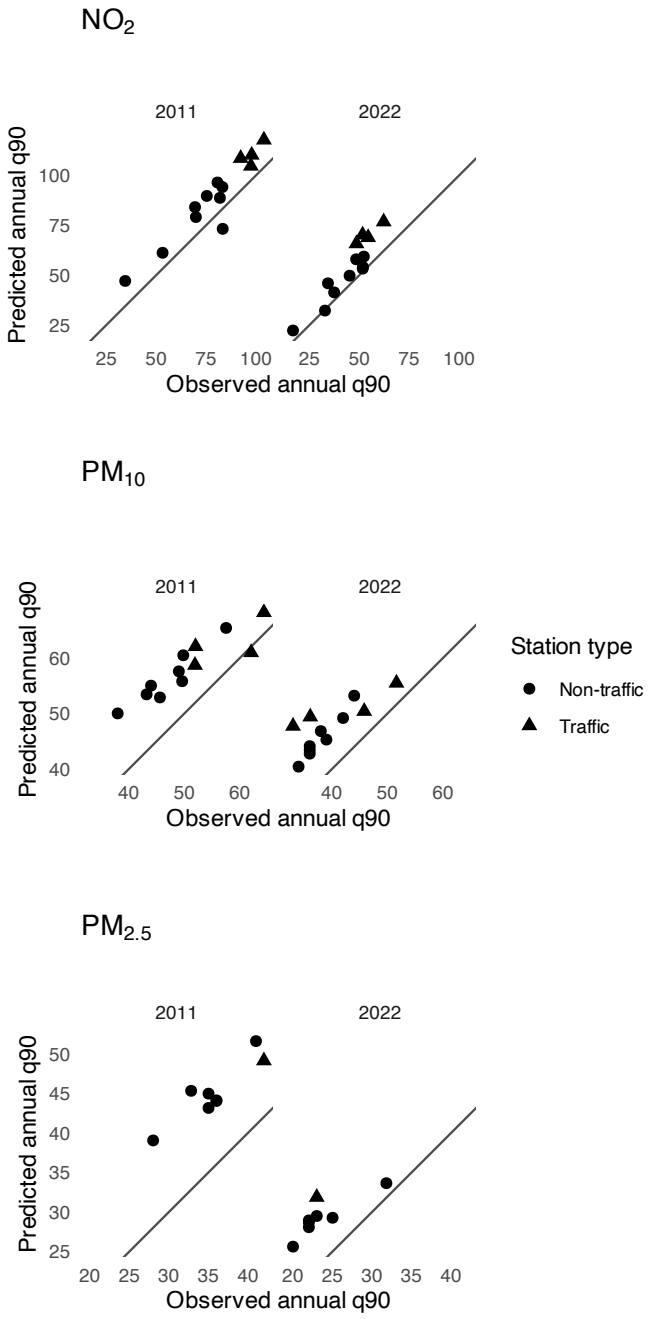

Fig. 6 Observed vs predicted annual quantiles for $\tau = 0.90$ in $\mu g/m^3$. The x-axis reports the empirical annual quantile of level $\tau = 0.90$ of daily mean concentrations, the y-axis reports the empirical annual 90-th quantile of the daily conditional $\tau = 0.90$ estimates evaluated at the corresponding station grid cell. Shape is given by recoded station type.

Table 55 Summary of differences between predicted and observed annual summaries for $\tau = 0.90$.

Pollutant	Year	Bias [min, max]
NO_2	2011	12.4 [−10.1, 16.2]
NO_2	2022	7.10 [−0.519, 18.6]
PM_{10}	2011	8.22 [−1.04, 12.0]
PM_{10}	2022	7.31 [3.87, 14.7]
$PM_{2.5}$	2011	9.05 [7.11, 12.5]
$PM_{2.5}$	2022	6.28 [1.83, 8.86]

Median and range [min, max] of $\widehat{q}^{0.90}_{\text{pred}} - q^{0.90}_{\text{obs}}$ computed across monitoring sites, where $q^{0.90}_{\text{obs}}$ is the empirical annual quantile of level $\tau = 0.90$ of daily mean concentrations and $\widehat{q}^{0.90}_{\text{pred}}$ is the annual 90-th quantile of the predicted daily conditional quantile of level $\tau = 0.90$ estimates at station locations.

9 $PM_{2.5}$ augmentation sensitivity

$PM_{2.5}$ and PM_{10} were strongly correlated in our dataset (Pearson's $r = 0.86$). Following established literature (e.g., Stafoggia et al. (2019, 2020)) and given the scarcity of $PM_{2.5}$ measurements, we conducted a supplementary sensitivity analysis by imputing $PM_{2.5}$ from PM_{10} concentrations via linear regression. This allowed us to augment the $PM_{2.5}$ network with four additional stations that did not originally measure $PM_{2.5}$.

9.1 Interpolation method

As presented in the main text, starting monitoring stations sample for $PM_{2.5}$ only included 8 stations, compared to the 12 measuring PM_{10}. Hence, Tiburtina, Fermi, Magna Grecia and Bufalotta stations concentrations were interpolated from PM_{10} values in the same period. Figure 7 is a descriptive tool that gives us a general idea of the linear relationship between the two particulate matters.

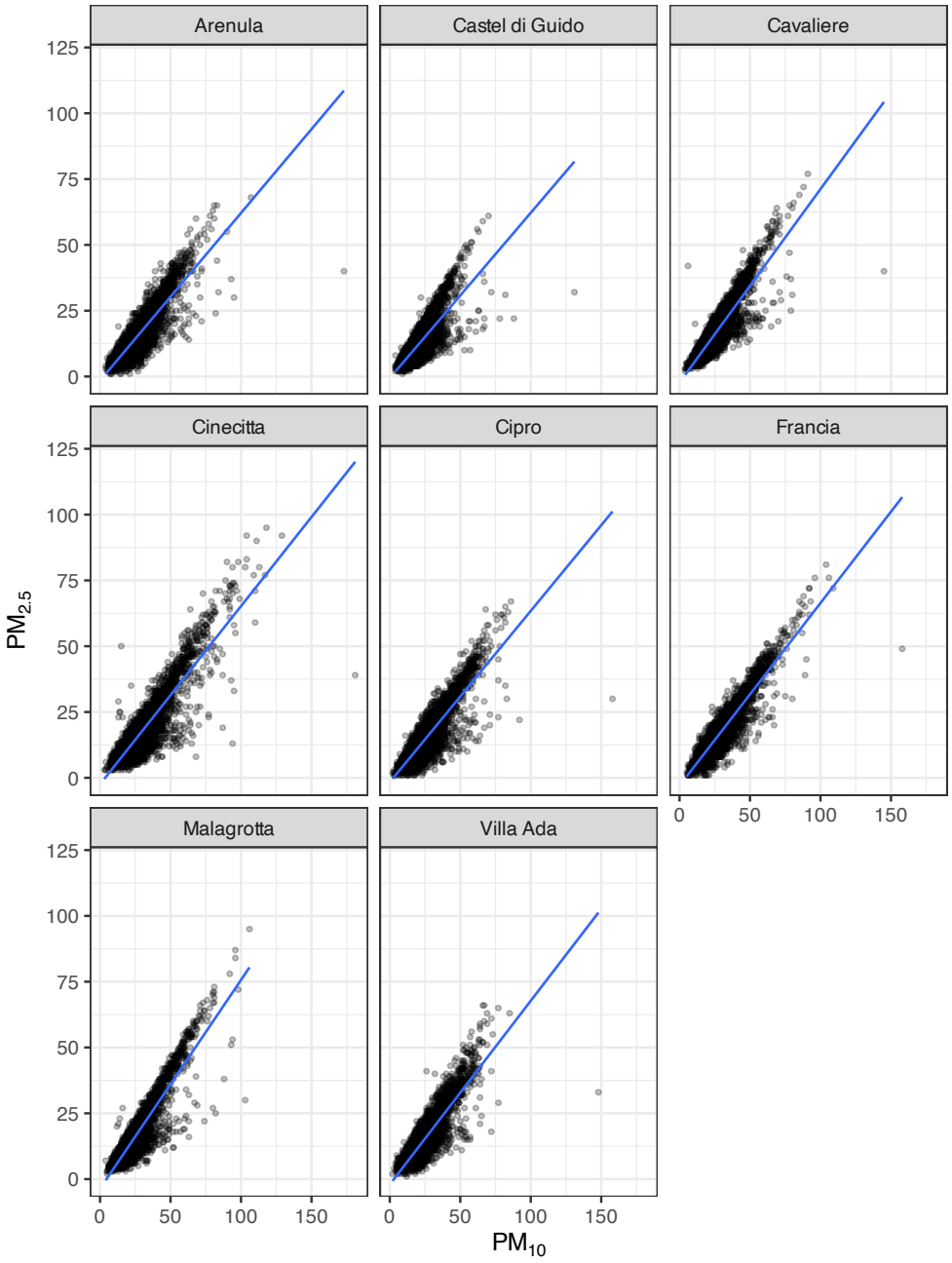

Fig. 7 Relationship between PM_{10} and $PM_{2.5}$ in shared monitoring sites. Original values in $\mu g/m^3$.

Hence, we performed an extremely rapid model selection comparing Akaike Information Criterion (AIC), and adjusted R^2. The best resulting model specification was:

$$\mathrm{PM}_{\mathbf{10}} + \mathrm{year} + \mathrm{wday} + \sin\left(\frac{\mathbf{2}\pi\,\mathrm{doy}}{\mathbf{365}}\right) + \cos\left(\frac{\mathbf{2}\pi\,\mathrm{doy}}{\mathbf{365}}\right) + \mathrm{x}_{\mathbf{std}} + \mathrm{y}_{\mathbf{std}}$$

The sin and cos terms capture daily seasonality patterns (with doy $\in \{1, \ldots, 365\}$), while wday $\in \{1, \ldots, 7\}$ the effect of weekly fluctuations. x_{std} and y_{std} represent the effect of spatial coordinates expressed in WGS 84 / UTM zone 32N and then normalised by their in sample maxima. In-sample fit for the selected model showed good results (0.258 RMSE, 0.193 MAE, adjusted $R^2 = 0.762$; computed on the $\log(1+x)$ scale).

9.2 Comparison measured-only vs augmented

To provide an example, Figure 8 displays the comparison for 2011 surface from the measured-only network (8 sites, on the left) with the surface obtained under the augmented network (8+4 sites, on the right in the same chart).The augmented fit seems to bring modest changes in spatial contrast, most notably around the Cinecitta station's area, in the east side of the city centre: the map seems slightly more discriminant around that pollution spike, probably due to the contribution of the newly added Tiburtina station. Nevertheless, the overall surface remains smooth. Given that the additional locations are indirectly obtained, in all cases these results should be interpreted cautiously and are reported only to evaluate the impact of network sparsity on $\mathrm{PM}_{2.5}$ mapping.

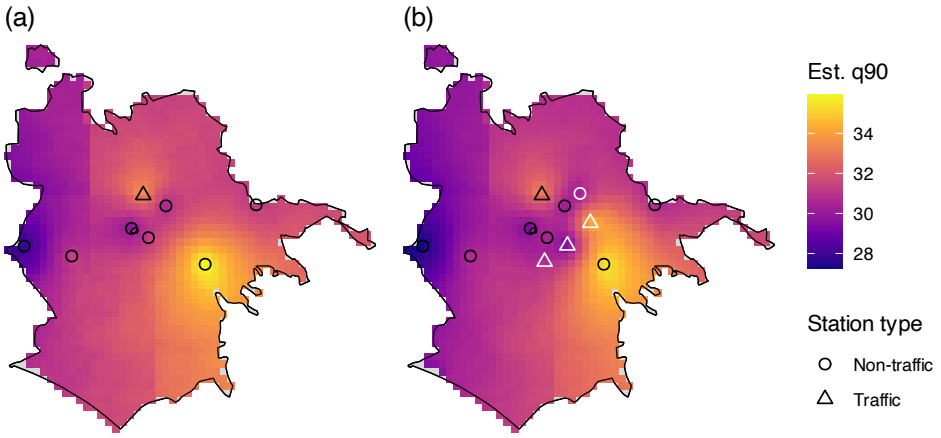

Fig. 8 Estimated quantile surfaces for $PM_{2.5}$ at $\tau = 0.90$. Values in $\mu g/m^3$. Annual averages of 2011 computed using (a) the measured-only network (8 sites), and (b) augmented network (8+4 sites, the latter in white).

References

Plummer M, Best N, Cowles K, et al (2006) Coda: Convergence diagnosis and output analysis for mcmc. R News 6(1):7–11. URL https://journal.r-project.org/archive/

Spiegelhalter DJ, Best NG, Carlin BP, et al (2002) Bayesian Measures of Model Complexity and Fit. Journal of the Royal Statistical Society Series B: Statistical Methodology 64(4):583–639. https://doi.org/10.1111/1467-9868.00353

Stafoggia M, Bellander T, Bucci S, et al (2019) Estimation of daily PM10 and PM2.5 concentrations in Italy, 2013–2015, using a spatiotemporal land-use random-forest model. Environment International 124:170–179. https://doi.org/10.1016/j.envint.2019.01.016

Stafoggia M, Johansson C, Glantz P, et al (2020) A Random Forest Approach to Estimate Daily Particulate Matter, Nitrogen Dioxide, and Ozone at Fine Spatial Resolution in Sweden. Atmosphere 11(3):239. https://doi.org/10.3390/atmos11030239